SCIENTIFIC REPORTS

OPEN

Clostridioides difficile LuxS mediates inter-bacterial interactions within biofilms

Received: 7 January 2019
Accepted: 21 June 2019
Published online: 09 July 2019

Ross T. Slater[1], Lucy R. Frost[1], Sian E. Jossi[1], Andrew D. Millard[2] & Meera Unnikrishnan[1]

The anaerobic gut pathogen, *Clostridioides difficile*, forms adherent biofilms that may play an important role in recurrent *C. difficile* infections. The mechanisms underlying *C. difficile* community formation and inter-bacterial interactions are nevertheless poorly understood. *C. difficile* produces AI-2, a quorum sensing molecule that modulates biofilm formation across many bacterial species. We found that a strain defective in LuxS, the enzyme that mediates AI-2 production, is defective in biofilm development *in vitro*. Transcriptomic analyses of biofilms formed by wild type (WT) and *luxS* mutant (*luxS*) strains revealed a downregulation of prophage loci in the *luxS* mutant biofilms compared to the WT. Detection of phages and eDNA within biofilms may suggest that DNA release by phage-mediated cell lysis contributes to *C. difficile* biofilm formation. In order to understand if LuxS mediates *C. difficile* crosstalk with other gut species, *C. difficile* interactions with a common gut bacterium, *Bacteroides fragilis*, were studied. We demonstrate that *C. difficile* growth is significantly reduced when co-cultured with *B. fragilis* in mixed biofilms. Interestingly, the absence of *C. difficile* LuxS alleviates the *B. fragilis*-mediated growth inhibition. Dual species RNA-sequencing analyses from single and mixed biofilms revealed differential modulation of distinct metabolic pathways for *C. difficile* WT, *luxS* and *B. fragilis* upon co-culture, indicating that AI-2 may be involved in induction of selective metabolic responses in *B. fragilis*. Overall, our data suggest that *C. difficile* LuxS/AI-2 utilises different mechanisms to mediate formation of single and mixed species communities.

Clostridiodes difficile (*Clostridium difficile*), an anaerobic, opportunistic pathogen, is the causative agent of *C. difficile* infection (CDI), a debilitating condition with symptoms ranging from mild diarrhoea to severe pseudomembranous colitis. ~453,000 cases of CDI were reported in the United States in 2011[1] and there have been increasing reports of CDI from different parts of the world[2–4]. Treatment of CDI is complicated by the fact that 20–36% of cases experience recurrence, relapsing after completion of initial treatment[5]. CDI is primarily a hospital-acquired infection with the elderly being at highest risk[6] and has been associated with the disruption of the gut microbiota as a result of the use of broad-spectrum antibiotics. However, more recently, there has been a reported increase in community-acquired cases where patients do not have the typical risk factors such as antibiotic exposure or recent hospitalisation[7].

Colonisation of *C. difficile* and development of CDI is influenced by composition of the native gut microbiota. Broadly, *Bacteroides*, *Prevotella*, *Bifidobacterium*, *Enterococcaceae* and *Leuconostocaceae spp*. correlate negatively[8–10], and Lactobacilli, *Aerococcaceae*, *Enterobacteriaceae*, and *Clostridium* correlate positively to *C. difficile* colonisation and disease[8,10–13]. While mechanisms underlying colonisation resistance are not entirely clear, some pathways have been described recently. Secondary bile acids produced by bacteria like *Clostridium scindens* can inhibit *C. difficile* growth, while other bile acids such as chenodeoxycholate can inhibit spore germination[14–16]. Studies have shown that the ability of *C. difficile* to utilise metabolites produced by the gut microbiota or mucosal sugars such as sialic acid promote *C. difficile* expansion in the gut[17,18]. However, gaps still remain in our understanding of *C. difficile* interactions with members of the gut microbiota.

Research into CDI has primarily focused on the action of two large toxins[19,20] that cause tissue damage, neutrophil recruitment and a severe inflammatory response[21]. More recently, a number of factors have been shown to influence adhesion of *C. difficile* to host cells and early colonisation, including cell wall proteins, adhesins and

[1]University of Warwick, Gibbet Hill Road, Coventry, CV4 7AL, United Kingdom. [2]University of Leicester, University Road, Leicester, LE1 7RH, UK. Correspondence and requests for materials should be addressed to M.U. (email: m.unnikrishnan@warwick.ac.uk)

flagella[22–26]. *C. difficile* also produces biofilms that confer increased resistance to antibiotics[27–29] and have recently shown to be associated with *C. difficile* infection *in vivo*, in close association with other commensal gut species[30].

Formation of adherent communities within the gut requires communication between bacteria. For many species, quorum sensing (QS) is important for the construction and/or dispersal of biofilm communities[31], with bacteria utilising diverse QS systems[31,32]. Many bacteria possess the metabolic enzyme LuxS, which is involved in the detoxification of S-adenoslylhomocysteine during the activated methyl cycle. Whilst catalysing the reaction of S-ribosylhomocysteine to homocysteine, LuxS produces the bi-product 4,5-dihydroxy-2,3-pentanedione (DPD). DPD is an unstable compound that spontaneously cyclises into several different forms. These ligands are collectively known as autoinducer-2 (AI-2), a group of potent, cross-species QS signalling molecules[33]. In many bacteria, including *C. difficile*, AI-2 plays a role in biofilm formation, with *luxS* mutants showing a defect during biofilm formation and development[27,34–39]. The precise mode of action for LuxS in *C. difficile* has remained elusive as a result of conflicting studies and the lack of a clear receptor for AI-2[34,40,41].

Here we investigate the role of LuxS within *C. difficile* and mixed biofilm communities. Interestingly, we find that *C. difficile* LuxS/AI-2 mediates the induction of two putative *C. difficile* R20291 prophages within *C. difficile* biofilms. In mixed biofilms, we show that in the presence of *B. fragilis*, a gut bacterium, *C. difficile* growth is inhibited and this inhibition is alleviated in the absence of LuxS. Dual species transcriptomics show that distinct metabolic pathways are triggered in mixed cultures with the wild type (WT) and *luxS* mutant *C. difficile* strains.

Results

LuxS mediates biofilm formation *in vitro*. We previously reported that a R20291 *C. difficile luxS* mutant (*luxS*) was defective in biofilm formation as measured by crystal violet (CV) staining[27]. However, in our subsequent studies, although we see a reduction in biofilms at 24 h, we observe a high variability in the WT biofilms formed at 24 h and in the reduction in the *luxS* mutant between experiments (Fig. 1A). Nevertheless, the biofilm defect for *luxS* was very consistent at later time points (72 h) (Fig. 1A,B). In spite of differences in total biofilm content, colony counts from the WT and *luxS* biofilms were similar at both time points (Fig. 1C). There were also no differences in the spore content of WT and *luxS* biofilms (~0.003% at 24 h and ~0.1% at 72 h) (Fig. S1).

To determine if AI-2 signalling is involved in biofilm formation, we first performed an AI-2 assay from both planktonic and biofilm supernatants as described by Carter *et al*. 2005 (Fig. S2A). AI-2 is produced maximally in mid-log and stationary phases as previously reported[40]. The WT strain produced less AI-2 in 24 h biofilms compared to log phase culture, while the *luxS* strain did not produce AI-2 as expected (Fig. S2B). To study if the reduction in biofilm formation in *luxS* could be complemented by chemically synthesised 4,5-dihydroxy-2, 3-pentanedione (DPD), the precursor of AI-2, was supplemented in the culture medium. Whilst high concentrations (>1000 nM) appeared to have only a partial effect on biofilm formation (Fig. S3), a concentration of 100 nM was capable of restoring the WT phenotype (Fig. 1D), indicating that AI-2 may be involved in signalling within *C. difficile* biofilms.

RNA-seq analysis reveals LuxS-mediated prophage induction. To investigate mechanism of action of LuxS/AI-2 in *C. difficile*, transcriptional profiles of *C. difficile* WT and *luxS* strains planktonically cultured (OD_{600} 0.8 in BHI) were first compared using RNA-seq. However, surprisingly, no differential transcriptional changes were observed (Accession number E-MTAB-7486). Following this, an RNA-seq analysis was performed with total RNA isolated from *C. difficile* WT and *luxS* biofilms grown in BHIS +0.1 M glucose [(BHIS-G) conditions used for biofilm assays in Fig. 1] for 18 h (Accession number E-MTAB-7523). Both strains show similar planktonic culture growth rates in BHIS-G as reported previously[27].

The DESeq2 variance analysis package[42] was used to identify genes that were differentially expressed in *luxS* ≥1.6-fold relative to the WT strain, with a p -adjusted value ≤0.05. This pairwise analysis identified 21 differentially expressed genes (Fig. 2A,C) (Table 1). Interestingly, all 18 down-regulated genes correspond to two prophage regions located within the *C. difficile* R20291 genome, CDR20291_1415–1464 and CDR20291_1197–1226 (Fig. 2B), as identified using the online phage search tool, Phaster[43,44]. A Fisher's exact test (p-value < 0.001 for both prophage regions) further confirmed an enrichment of differently regulated genes in prophage regions. There were only three genes upregulated in the *luxS* biofilms compared to the WT; two of these were involved in trehalose utilisation, while the third was a phosphotransferase system glucose-specific transporter.

To demonstrate the presence of phage in the biofilm, cell-free supernatants were treated with DNase, before a subsequent DNA extraction was performed. As the bacterial cells were already removed, only DNA within intact bacteriophages would be protected from DNase. A 16S rRNA gene PCR was performed to confirm digestion of all free extracellular genomic DNA from the biofilm (Fig. 3A). PCRs with primers corresponding to genes specific to each prophage, confirmed that the DNA extracted had come from the phage (Fig. 3B). Since cell lysis is linked to phage release, we quantified and compared the total extracellular DNA (eDNA) content of *luxS* mutant and WT biofilms. The WT biofilms contained more eDNA compared to the *luxS* mutant at 24 h and 72 h (Fig. 3C). Overall, these data suggest that AI-2 may play a role in inducing prophages in *C. difficile* biofilms, which leads to phage-mediated host cell lysis and eDNA generation, which may contribute to subsequent biofilm accumulation.

***C. difficile* is inhibited when cultured with *B. fragilis* in mixed biofilms.** Given the high microbial density within the gut, *C. difficile* likely needs to interact with other members of the gut microbiota to establish itself within this niche. As an inter-species signalling function has been previously proposed for AI-2[45], we sought to investigate the interactions between a gut-associated *Bacteroides spp* and *C. difficile*. We examined *C. difficile* interactions with *Bacteriodes fragilis*, a gut commensal and pathogen, that has been previously reported to negatively correlate with CDI infections[46].

C. difficile formed significantly more biofilms *in vitro* compared with *B. fragilis* in monocultures, as measured by CV staining (Fig. 4A). When both organisms were co-cultured, less biofilm was formed compared to

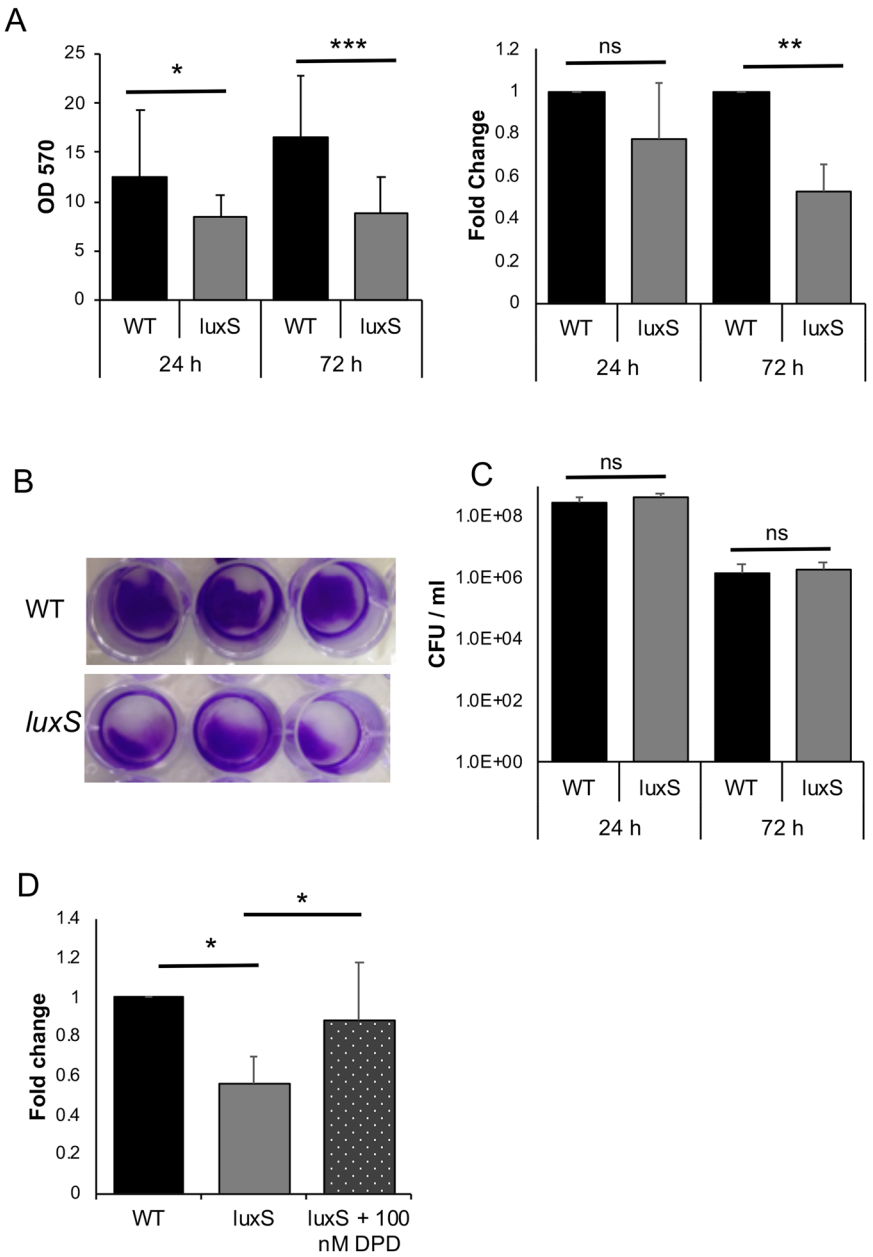

Figure 1. *LuxS* biofilm defect is reversed by addition of DPD. (**A**) WT and *LuxS* biofilms were grown for 24 h or 72 h and stained with 0.2% CV, followed by measuring OD_{570}, N = 5. (**B**) Representative pictures of crystal violet stained *C. difficile* WT and *luxS* biofilms after 72 h. (**C**) Colony counts (vegetative cells) from biofilms (N = 7) after 24 h and 72 h. (**D**) The AI-2 precursor, DPD, was exogenously supplemented to *LuxS* at a concentration of 100 nM, followed by biofilm staining and quantitation with 0.2% CV after 72 h (N = 4). Error bars indicate SD, $*p < 0.05$, $**p < 0.01$, $***p < 0.001$ as determined by Student's t-test or by Mann-Whitney U test, ns- not significant.

C. difficile monoculture (Fig. 4A). Both *B. fragilis* and *C. difficile* grow well, although with slightly different growth rates, in BHIS-G (Fig. S4). To investigate the impact of co-culturing on both *C. difficile* and *B. fragilis*, bacterial numbers (CFU/ml) were determined from monoculture and mixed biofilms (Fig. 4B). Colony counts obtained from the mono and co-culture biofilms confirmed that *B. fragilis* was a poor biofilm producer when cultured alone. Interestingly, when both species were co-cultured, the CFU/ml for *C. difficile* was significantly reduced, and the CFU/ml of *B. fragilis* was significantly higher. This reduction of colony counts of *C. difficile* was observed at both 24 h (Fig. 4B) and 72 h (Fig. S5). AI-2 production from single and mixed biofilms was also quantitated. We observed no production of AI-2 by *B. fragilis*, and a reduction of AI-2 production by the mixed biofilms compared with the WT *C. difficile* biofilms (Fig. S6). *C. difficile* spore measurements from the mixed biofilms indicate that while the percentage of spores is higher (2%) due to the decrease in *C. difficile* numbers, there was no

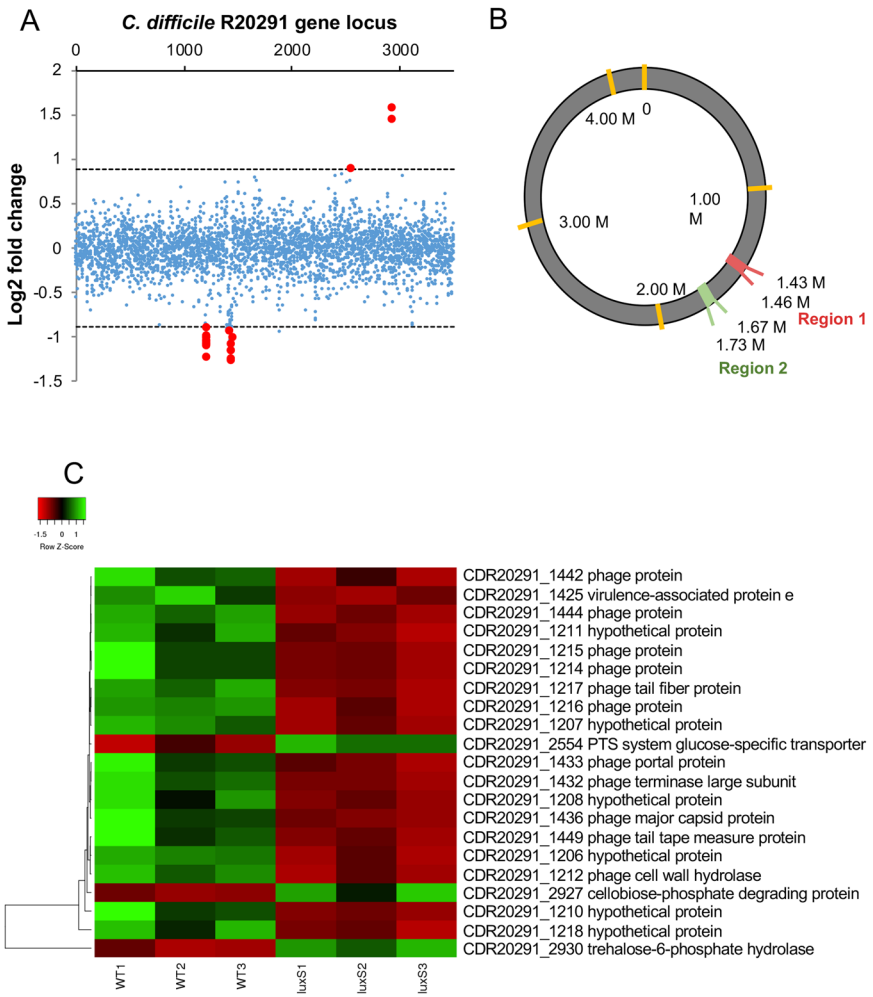

Figure 2. Down-regulation of prophage genes in the *C. difficile luxS* mutant. (**A**) Pairwise analysis identified 21 differentially expressed genes in *luxS* (red points). All 18 down-regulated genes clustered into two regions. (**B**) Three prophage regions are identified in the *C. difficile* genome using Phaster. Regions 2 and 3 were down regulated in *luxS*. (**C**) Heat map representation of the genes that were differentially expressed in *luxS,* red and green indicate down- and up-regulation respectively when compared to WT. 18 prophage genes were found to be down-regulated in *luxS* relative to WT, whilst two genes involved in trehalose metabolism were up-regulated in *luxS* relative to WT. Data shown is the mean of 3 independent experiments in triplicates. Differential expression was defined as $\geq$1.6-fold change relative to WT with an adjusted *p*-value $\leq$ 0.05.

increase in the actual spore numbers (Fig. S7). These data suggest that the presence of *B. fragilis* in biofilms results in inhibition of *C. difficile* growth.

To understand if the inhibitory effect was due to a factor secreted by *B. fragilis*, *C. difficile* and *B. fragilis* were co-cultured under planktonic conditions for 6 h and 10 h (Fig. 4C). However, there were no significant differences in *C. difficile* bacterial numbers between mono and co-culture. Additionally, supplementing biofilms with *B. fragilis* planktonic or biofilm culture supernatants did not cause *C. difficile* growth inhibition (Fig. S8), indicating that the observed inhibitory effects were specific to adherent biofilms i.e. when they are in close proximity to each other.

LuxS is involved in the *B. fragilis* inhibition of *C. difficile*. To study the role of LuxS in *C. difficile*-*B. fragilis* interactions, WT *C. difficile* and *luxS* strains were co-cultured with *B. fragilis* in mixed biofilms. CV staining of biofilms showed that there was less *luxS* biofilm formed compared to the WT when co-cultured with *B. fragilis* (Fig. 5A). While colony counts of *C. difficile* in monocultures were similar for both WT and *luxS* strains (Fig. 1B), when co-cultured with *B. fragilis* the bacterial counts for both *C. difficile* strains were significantly reduced, although the reduction was significantly higher for the WT than *luxS* (Fig. 5B). Colony counts for *B. fragilis* increased significantly during co-culture, with similar levels observed in both co-culture conditions (Fig. 5B). There was no increase in the spore numbers in the *luxS* in mixed biofilms (Fig. S7). These data suggest that AI2/LuxS is involved in mediating the *B. fragilis*-induced inhibition of *C. difficile*, when they are within adherent communities.

No	Gene ID	log2 FoldChange	Gene annotation
1	CDR20291_1206	−0.994213972	hypothetical protein
2	CDR20291_1207	−1.059645046	hypothetical protein
3	CDR20291_1208	−1.227114763	hypothetical protein
4	CDR20291_1210	−1.08584066	hypothetical protein
5	CDR20291_1211	−1.0763802	hypothetical protein
6	CDR20291_1212	−1.009946545	phage cell wall hydrolase
7	CDR20291_1214	−1.09972952	phage protein
8	CDR20291_1215	−1.038498251	phage protein
9	CDR20291_1216	−1.047731727	phage protein
10	CDR20291_1217	−0.999294901	phage tail fiber protein
11	CDR20291_1218	−0.898724949	hypothetical protein
12	CDR20291_1425	−0.928686375	virulence-associated protein e
13	CDR20291_1432	−1.243533992	phage terminase large subunit
14	CDR20291_1433	−1.154529376	phage portal protein
15	CDR20291_1436	−1.156306053	phage major capsid protein
16	CDR20291_1442	−1.085573967	phage protein
17	CDR20291_1444	−1.257181603	phage protein
18	CDR20291_1449	−1.008627768	phage tail tape measure protein
19	CDR20291_2554	0.895993497	PTS system glucose-specific transporter subunit IIA
20	CDR20291_2927	1.587075038	cellobiose-phosphate degrading protein
21	CDR20291_2930	1.444846424	trehalose-6-phosphate hydrolase

Table 1. *Genes up- and down-regulated in* luxS *relative to the WT C. difficile* Note: P-adjusted value ≤ 0.05.

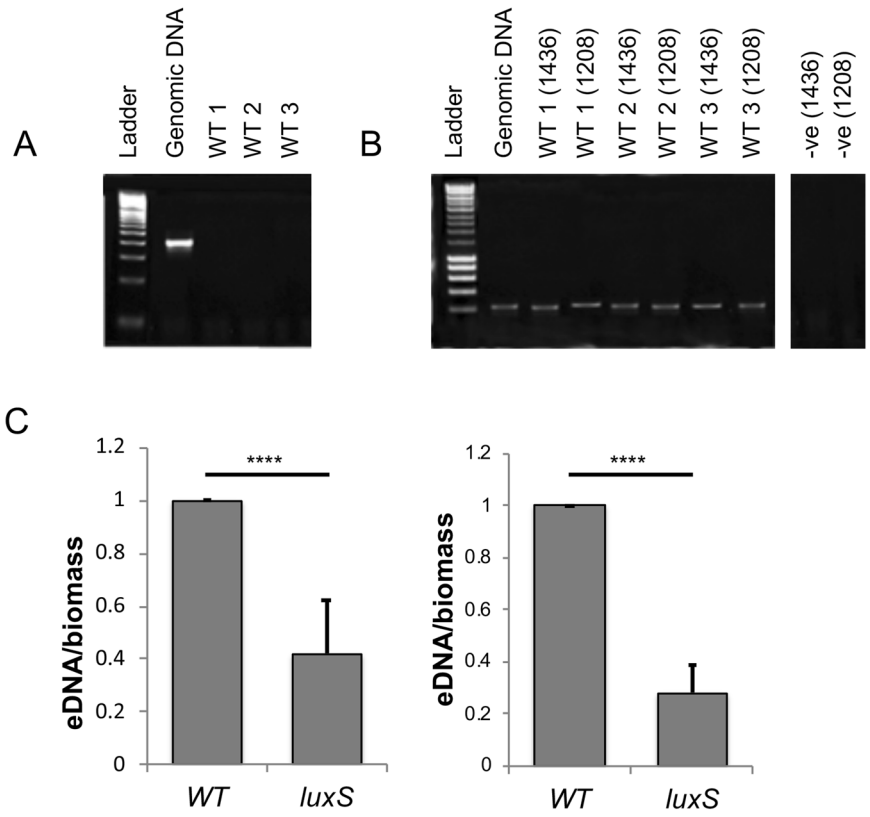

Figure 3. Presence of phage and eDNA in *C. difficile* biofilms. The phage origin of DNA isolated from WT biofilms was confirmed by PCR, using primers for 16S (**A**) and two phage genes (CDR20291_1436 and CDR20291_1208) (**B**). The negative controls were run on a different part of the same gel. The gel pictures were trimmed with no adjustment to the intensities. WT-1–3 are three biological replicates. (**C**) Total eDNA extracted from the WT and *luxS* mutant biofilms after 24 h and 72 h, normalised to the biofilm biomass. N = 3, ****$p < 0.0001$ as determined by Mann-Whitney U test.

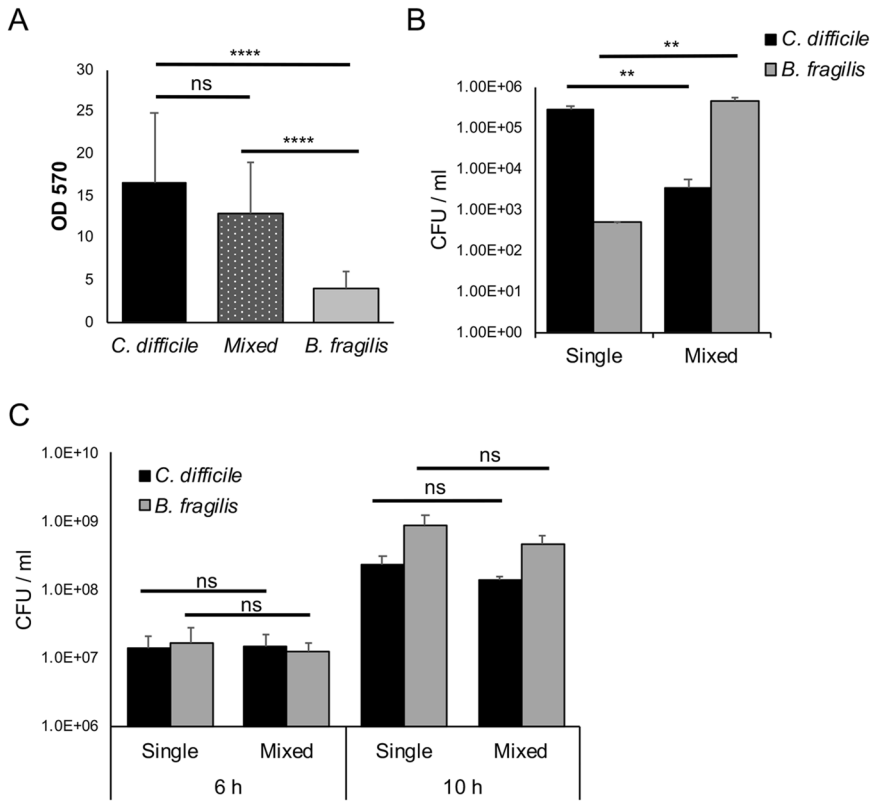

Figure 4. *B. fragilis* mediated inhibition of *C. difficile* in mixed biofilms. (**A**) Biofilm of *C. difficile*, *B. fragilis* and both species co-cultured (mixed) were grown for 24 h and stained with 0.2% CV, followed by measuring OD_{570}. (**B**) Colony counts for both *C. difficile* (vegetative cells) and *B. fragilis* from mono and co-culture biofilms after 24 h. (**C**) Colony counts for both *C. difficile* (vegetative cells) and *B. fragilis* from mono and co-culture during planktonic growth. Data shown is the mean of 3 independent experiments in triplicates and error bars indicate SD, $**p < 0.005$, $****p < 0.0001$ as determined by one-way ANOVA, Tukey's multiple comparison test, ns -not significant (significant differences were determined for *C. difficile* or *B. fragilis* mean CFU counts between single and mixed biofilms).

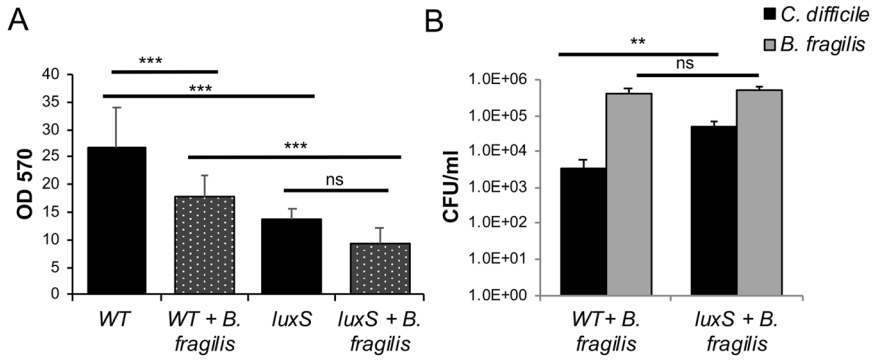

Figure 5. *B. fragilis*-mediated inhibition of *C. difficile* is more prominent for WT than *LuxS*. (**A**) Biofilms for mono and co-cultures of *C. difficile* WT and *luxS* with *B. fragilis* were grown for 24 h and stained with 0.2% CV and were quantified using a spectrophotometer OD_{570}. (**B**) Colony counts for *C. difficile* WT, *C. difficile luxS* (vegetative cells) during co-culture with *B. fragilis* were performed at 24 h. Data shown is the mean of 3 independent experiments in triplicates and error bars indicate SD, $**p < 0.01$, $***p < 0.001$ as determined by one-way ANOVA, Tukeys multiple comparison test (significant differences were determined for *C. difficile* or *B. fragilis* mean CFU counts between single and mixed biofilms).

Dual species RNA-seq analysis shows altered metabolism in *C. difficile* and *B. fragilis* in the absence of LuxS. To investigate mechanisms underlying the *C. difficile* inhibition mediated by *B. fragilis*, we performed an RNA-seq analysis to compare biofilm monocultures of *C. difficile* WT, *luxS* or *B. fragilis* with mixed

biofilm co-cultures of *C. difficile* WT or *luxS* with *B. fragilis* (Accession number E-MTAB-7523). Differentially expressed genes were defined as having ≥1.6-fold relative to their respective control (mono-cultures of either *B. fragilis* or *C. difficile* WT), with an adjusted *p*-adjusted value ≤ 0.05.

We compared the expression profiles of *C. difficile* WT biofilms to *C. difficile* WT-*B. fragilis* mixed biofilms and *C. difficile luxS* biofilms to *C. difficile luxS*-*B. fragilis* mixed biofilms. A total of 45 genes were up-regulated (21) or down-regulated (24) in *C. difficile* WT (Fig. 6, Table 2), while 69 genes were differentially expressed in *C. difficile luxS* of which 34 were down-regulated and 35 up-regulated, during co-culture with *B. fragilis* (Fig. 6A, Table 3).

Eight up-regulated genes were specific to *C. difficile* WT co-culture (Table 2). Of these, four genes involved in fatty acid biosynthesis and metabolism: *fabH* encoding 3-oxoacyl-[acyl-carrier protein] synthase III, *fabK* encoding trans-2-enoyl-ACP reductase, *accC* encoding a biotin carboxylase (acetyl-CoA carboxylase subunit A), and *accB* encoding a biotin carboxyl carrier protein of acetyl-CoA carboxylase (Table 2). 11 genes were down-regulated exclusively in WT however, these genes do not coincide with a specific metabolic pathway.

18 up-regulated genes were specific to *luxS* in co-culture (Table 3). These include a putative homocysteine S-methyltransferase, a putative osmoprotectant ABC transporter, substrate binding/ permease protein, ribonucleoside-diphosphate reductase alpha chain (*nrdE*) and two genes from the trehalose operon: a PTS system II ABC transporter, and trehalose-6-phosphate hydrolase (treA). 24 genes were down-regulated (Table 3), which include 3 genes involved in thiamine metabolism *thiD*, *thiK* and *thiE1*, (CDR20291_1497, CDR20291_1498 and CDR20291_1499 respectively) which encode a putative phosphomethylpyrimidine kinase, 4-methyl-5 -beta-hydroxyethylthiazole kinase and thiamine-phosphate pyrophosphorylase respectively.

A total of 26 genes were differentially expressed in both *C. difficile* WT and *C. difficile luxS* when co-cultured with *B. fragilis* (Fig. 6A, Table S1). These include six up-regulated genes (*accB*, *abfH*, *abfT*, *abfD*, *sucD* and *cat1*) involved in carbon and butanoate metabolism, with *cat1*, which encodes succinyl-CoA:coenzyme A transferase, being the highest up-regulated gene for both *C. difficile* strains.

When *C. difficile* WT-*B. fragilis* mixed biofilms and *luxS*-*B. fragilis* mixed biofilms were compared to *B. fragilis* single biofilms, in contrast, a higher number of genes (266) were differentially expressed in *B. fragilis* when co-cultured with *C. difficile* (WT and *luxS*) (Table S4, Fig. 6B). A total of 114 *B. fragilis* genes were found to be specific to *C. difficile* WT co-culture, with 56 of these up-regulated and 58 down-regulated (Table S2). Similarly, 91 genes were found to be specific to *C. difficile luxS* co-culture, with 56 of these up-regulated and 35 down-regulated (Table S3). Although distinct *B. fragilis* expression profiles were observed with the WT and *luxS* (Fig. 6B), there were no clear pathways identified in the datasets.

Whilst the highest up-regulated gene in both WT and LuxS co-cultures encodes a putative virus attachment protein, no other viral genes were shown to be up-regulated (Table S4). Genes encoding iron containing proteins desulfoferrodoxin and rubrerythrin were highly up-regulated in both conditions. Interestingly, multiple copies of *fecR*, a key regulator for the ferric citrate transport system[47], and ferrous iron transport protein B were also up-regulated. Additionally, a number of other metabolic pathways were up-regulated, including four genes (encoding 3-isopropylmalate dehydratase small subunit, 3-isopropylmalate dehydrogenase, Galactokinase and 3-isopropylmalate dehydratase large subunit) involved in valine, leucine and isoleucine biosynthesis and C5-branched dibasic acid metabolism. It should be noted that many of the up-regulated genes were hypothetical proteins of unknown function. Similarly, several metabolic pathways were down-regulated in both co-culture conditions. These include six genes involved in carbon metabolism, four genes involved in alanine, aspartate and glutamate metabolism, and four genes involved in the biosynthesis of amino acids, although these appear to be single genes rather than specific pathways.

Discussion

Inter-bacterial interactions within gut communities are critical in controlling invasion by intestinal pathogens. Quorum sensing molecules such as AI-2 are instrumental in bacterial communication, especially during formation of bacterial communities[31,36,37,48–50]. *C. difficile* produces AI-2, although the mechanism of action of LuxS/AI-2 in *C. difficile*, particularly within a biofilm community is unclear. We report here that the *C. difficile* LuxS/AI-2 plays an important role in the formation of single and multi-species communities. In *C. difficile* biofilms, LuxS mediates the induction of prophages, which likely contributes to the biofilm structure. Whereas, in a mixed biofilm of *C. difficile* and the intestinal commensal and pathogen, *B. fragilis*, LuxS likely triggers the induction of differential metabolic responses in *B. fragilis*, that leads to growth inhibition of *C. difficile*. To our knowledge, this is the first time dual species RNA-seq[51] has been applied to analyse interactions between anaerobic gut bacteria in an adherent biofilm community.

Bacterial biofilms contain a number of extracellular components that make up their complex structure including extracellular DNA (eDNA), a key component that binds together bacteria within a community. Autolysis is a common mechanism by which eDNA is released from bacterial cells[52]. In bacteria such as *Staphylococcus aureus* and *Pseudomonas aeruginosa*, eDNA is generated through the lysis of subpopulations within a biofilm, under the control of quorum sensing[52–55]. In *C. difficile luxS* mutant (*luxS*) biofilms, we observe reduced induction of two *C. difficile* prophages compared with the WT. These phage loci were conserved in several *C. difficile* strains with the Region 2 encoding a phiC2-like, phi-027 phage[56–58]. Given that it has previously been shown that eDNA is a major component of *C. difficile* biofilms[27,30], it is likely that phage-mediated bacterial cell lysis and subsequent DNA release help build a biofilm. Indeed, given the detection of eDNA in the *luxS* biofilms, there are likely other unknown eDNA release mechanisms during *C. difficile* biofilm formation.

Phages are also known to control biofilm structure in some organisms: a filamentous phage of *P. aeruginosa* was reported to be a structural component of the biofilm[59] and an AI-2 induced phage mediated the dispersal of *Enterococcus faecalis* biofilms[60]. Although attempts to visualise phages from *C. difficile* biofilms with transmission electron microscopy (data not shown) were unsuccessful, we cannot rule out the possibility that *C. difficile* phages may directly influence the biofilm structure. While the precise mechanisms by which LuxS/AI-2 controls phage

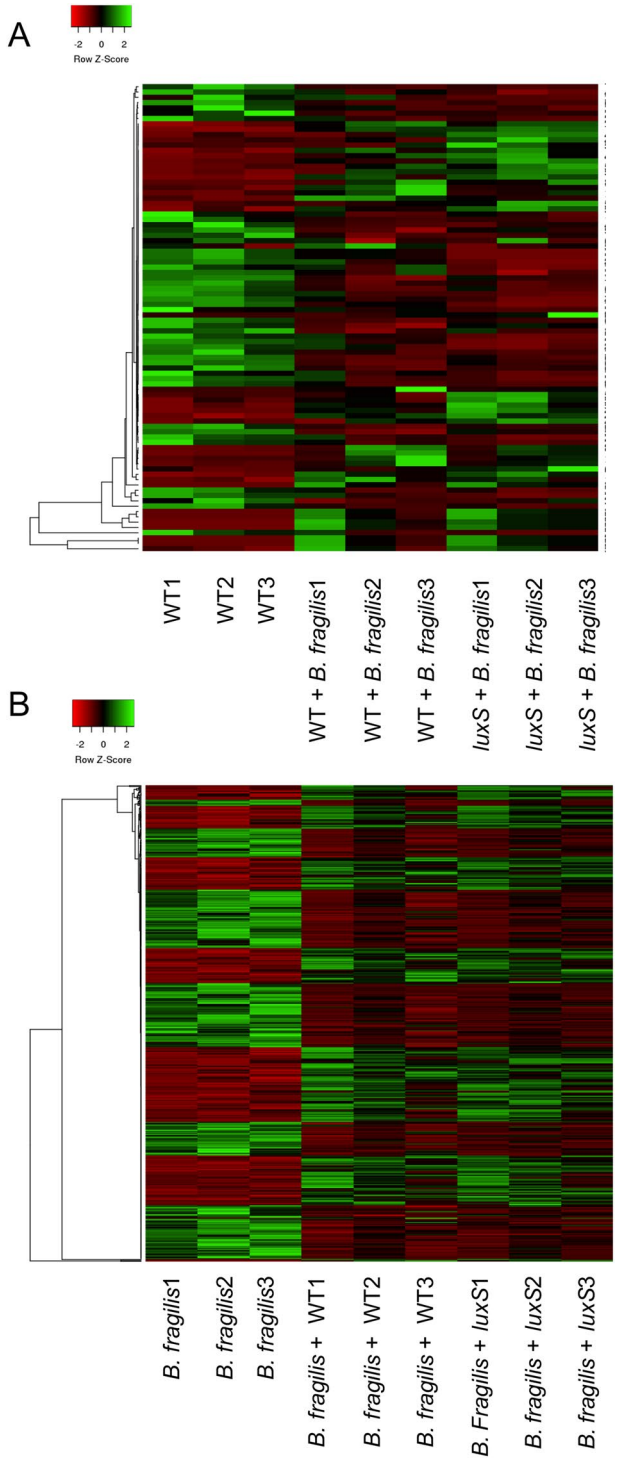

Figure 6. Dual species RNA-seq shows modulation of metabolic pathways in *C. difficile* WT, *luxS* and *B. fragilis*. Heat maps showing clustering of up- and down-regulated genes in (**A**) *C. difficile* WT and *luxS* co-cultured with *B. fragilis* compared to *C. difficile* WT mono-culture, and in (**B**) *B. fragilis* co-cultured with *C. difficile* WT and *luxS* compared to *B. fragilis* mono-culture. Red indicates genes that are down-regulated, whilst green indicates genes that are up-regulated.

induction are yet to be elucidated, AI-2 appears to be signalling through a yet unidentified AI-2 receptor in *C. difficile*. Phage-mediated control of biofilms may in part explain the variation observed in biofilm formation between different *C. difficile* strains[61].

The human gut hosts a variety of bacterial species, which compete or coexist with each other. It is likely that the bacteria occupying this niche form multi-species bacterial communities in association with the mucus layer. Interactions within such communities are important in gaining a better understanding of phenomena such as

No	Gene ID	log2FoldChange	Gene Annotation
1	CDR20291_0194	1.3822081	10 kDa chaperonin
2	CDR20291_1016	1.7087847	glycerol-3-phosphate acyltransferase PlsX
3	CDR20291_1017	1.7011992	3-oxoacyl-ACP synthase III
4	CDR20291_1018	1.2469326	trans-2-enoyl-ACP reductase
5	CDR20291_1337	1.3290499	transcriptional regulator
6	CDR20291_1861	1.412304	biotin carboxylase acetyl-CoA carboxylase subunit A
7	CDR20291_2027	1.6309458	2-nitropropane dioxygenase
8	CDR20291_3225	1.0229025	formate/nitrite transporter
9	CDR20291_0363	−1.377088	radical SAM protein
10	CDR20291_0364	−1.003595	hypothetical protein
11	CDR20291_0365	−1.461207	(R)-2-hydroxyisocaproate dehydrogenase
12	CDR20291_0659	−1.248536	radical SAM protein
13	CDR20291_1271	−1.15672	hypothetical protein
14	CDR20291_1309	−1.208811	phosphohydrolase
15	CDR20291_1400	−1.833327	imidazole glycerol phosphate synthase subunit HisH
16	CDR20291_1834	−1.411634	ethanolamine/propanediol ammonia-lyase heavy chain
17	CDR20291_2416	−1.231651	hypothetical protein
18	CDR20291_2417	−1.574982	hypothetical protein
19	CDR20291_2610	−1.046807	two-component sensor histidine kinase

Table 2. Genes up and down-regulated in WT during co-culture with *B. fragilis relative to the* WT *C. difficile* monoculture. Note: P-adjusted value ≤ 0.05.

'colonisation resistance' which prevents pathogens such as *C. difficile* from establishing an infection[14]. Whilst sequencing studies have identified members of the *Bacteroides* genus as being associated with gut colonisation resistance to *C. difficile*, the mechanisms have remained elusive[10]. A recent study demonstrated that production of the enzyme: bile salt hydrolase, is responsible for the inhibitory effect of *B. ovatus* on *C. difficile*[62]. This study reported that in the presence of bile acids, cell free supernatants for *B. ovatus* were capable of inhibiting the growth of *C. difficile* whereas in the absence of bile acids, *C. difficile* growth was promoted. Since bile acids are not supplemented into our media, a different mechanism is likely responsible for *B. fragilis* mediated inhibition of *C. difficile*. Also, the growth restraining effects of *B. fragilis* on *C. difficile* were evident only within mixed biofilms, not in planktonic culture or with culture supernatants. While it is likely that cell-cell contact is essential for the inhibitory effect, we cannot exclude involvement of an inhibitory secreted molecule that accumulates to a higher concentration within a biofilm environment, or that *B. fragilis* has a competitive growth advantage in a biofilm environment.

A dual species RNA-seq analysis performed to understand the interactions between the two bacterial species, showed that largely all the differentially expressed genes mapped to distinct metabolic pathways. Overall, a higher number of genes were modulated in *B. fragilis* as compared to *C. difficile* strain during co-culture, which is in line with the growth characteristics observed. Carbon and butanoate metabolism pathways were induced in *C. difficile* strains in response to co-culture (*accB*, *abfH*, *abfT*, *abfD*, *sucD* and *cat1*). An up-regulation of the succinate utilisation genes was also recently reported in *C. difficile* 630 microfermenter biofilm cells as compared to planktonic cells[63]. As *B. fragilis* is known to produce succinate[64], it is likely that the upregulation in these pathways results from the increased levels of succinate in the culture medium. However, since gut microbiota-produced succinate promotes *C. difficile* growth *in vivo*[17], it is unlikely that these changes are directly responsible for the observed inhibition of *C. difficile*. However, bacteria utilise carbohydrates in a sequential manner[65]. Consistent with this, we observed a down-regulation of genes important for the utilisation of pyruvate such as *bcd2* and *idhA* encoding for butyryl-CoA dehydrogenase and (r)-2-hydroxyisocaproate dehydrogenase respectively. A down-regulation of sugar fermentation pathway genes was also observed by Poquet *et al.* in single species *C. difficile* biofilms compared to planktonic cultures[63]. Such a shift in metabolism could allow *B. fragilis* to fully consume other metabolites, and thus enabling it to outcompete *C. difficile*.

Additionally, it is interesting to note that a number of copies of the ferric citrate transport system regulator, *fecR*, are up-regulated in *B. fragilis* during *C. difficile* co-culture. The ferric citrate transport system is an iron uptake system that responds to the presence of citrate[47,66]. Analysis of the *C. difficile* genome using BLAST (NCBI) showed that *C. difficile* does not possess this iron uptake system. Given the evidence that ferric citrate is an iron source in the gut[47,67], *B. fragilis* may have an advantage over *C. difficile* in sequestering iron, and thus preventing *C. difficile* colonisation. Although the clear modulation of metabolic pathways strongly suggest a competitive advantage of *B. fragilis* over *C. difficile*, it is possible that the genes with unknown functions that are differentially expressed in *B. fragilis* (Table S1), encode pathways for the production of yet to be identified small inhibitory molecules.

The LuxS/AI-2 quorum sensing system is known to have a cross-species signalling role in many bacteria[45,68]. While all sequenced *C. difficile* strains produce AI-2, only selected strains of *B. fragilis* have the ability to produce AI-2[69]. A recent study showed that *Ruminococcus obeuem* inhibited *Vibrio cholerae* in the gut via LuxS/AI-2 mediated downregulation of *V. cholerae* colonisation factors[70]. Also, AI-2 produced by engineered *E. coli* was

No	Gene ID	log2FoldChange	Gene Annotation
1	CDR20291_0491	1.0964355	RNA methylase
2	CDR20291_0492	1.1802034	hypothetical protein
3	CDR20291_0493	1.0076105	outer membrane lipoprotein
4	CDR20291_0715	1.6245725	N-acetylmuramoyl-L-alanine amidase
5	CDR20291_1366	0.9274027	ferrous ion transport protein
6	CDR20291_1374	1.1651176	iron-sulfur protein
7	CDR20291_1691	1.4187304	nitrite and sulfite reductase subunit
8	CDR20291_1716	1.3143654	thiol peroxidase
9	CDR20291_1717	1.110872	hypothetical protein
10	CDR20291_1934	1.5456229	hypothetical protein
11	CDR20291_1936	1.3368874	GntR family transcriptional regulator
12	CDR20291_1937	1.3736945	ABC transporter ATP-binding protein
13	CDR20291_2389	1.2619709	competence protein
14	CDR20291_2830	1.11333	ribonucleoside-diphosphate reductase subunit alpha
15	CDR20291_2928	1.7538156	PTS system transporter subunit IIABC
16	CDR20291_2930	1.5713168	trehalose-6-phosphate hydrolase
17	CDR20291_3075	1.3649687	osmoprotectant ABC transporter substrate-binding/permease
18	CDR20291_3104	0.8099098	sigma-54-dependent transcriptional activator
19	CDR20291_3434	1.4402419	homocysteine S-methyltransferase
20	CDR20291_0025	−1.32053	acetoin:2%2C6-dichlorophenolindophenol oxidoreductase subunit alpha
21	CDR20291_0615	−0.86915	nucleotide phosphodiesterase
22	CDR20291_0802	−2.260047	ABC transporter substrate-binding protein
23	CDR20291_0911	−1.24181	electron transfer flavoprotein subunit beta
24	CDR20291_1359	−0.850952	hypothetical protein
25	CDR20291_1370	−1.124726	tyrosyl-tRNA synthetase
26	CDR20291_1497	−1.456296	phosphomethylpyrimidine kinase
27	CDR20291_1498	−1.727285	hydroxyethylthiazole kinase
28	CDR20291_1499	−1.276387	thiamine-phosphate pyrophosphorylase
29	CDR20291_1591	−1.51799	dinitrogenase iron-molybdenum cofactor
30	CDR20291_1901	−1.832663	ABC transporter ATP-binding protein
31	CDR20291_1902	−1.875507	ABC transporter substrate-binding protein
32	CDR20291_1903	−1.659329	ABC transporter permease
33	CDR20291_1904	−1.638609	hypothetical protein
34	CDR20291_1925	−1.54806	flavodoxin
35	CDR20291_2474	−1.434272	DNA-directed RNA polymerase subunit omega
36	CDR20291_2515	−1.603951	amino acid permease family protein
37	CDR20291_2516	−1.176482	cobalt dependent x-pro dipeptidase
38	CDR20291_2660	−0.958814	teichuronic acid biosynthesis glycosyl transferase
39	CDR20291_2870	−2.335518	hypothetical protein
40	CDR20291_3142	−1.665916	pyrroline-5-carboxylate reductase
41	CDR20291_3143	−1.830481	formate acetyltransferase
42	CDR20291_3144	−1.643573	pyruvate formate-lyase 3 activating enzyme

Table 3. Genes up and down-regulated in *luxS* during co-culture with *B. fragilis relative to the* WT *C. difficile* monoculture. Note: P-adjusted value ≤ 0.05.

reported to influence firmicutes/bacteroidetes ratios in microbiota treated with streptomycin[71]. Our data show the involvement of LuxS/AI-2 in the *B. fragilis*-mediated *C. difficile* growth inhibition. As the *B. fragilis* strain used in this study does not produce AI-2, it is likely that *B. fragilis* responds differentially to AI-2 produced by *C. difficile*. Similar to the WT, most transcriptional changes were in metabolic pathways, although specific sets of genes were modulated in the *luxS* mutant. Modulation of prophage genes was not seen, unlike single biofilm cultures, indicating different dominant mechanisms at play in a multi-species environment.

It was interesting to note that the trehalose utilisation operon, which provides a growth advantage to *C. difficile* against other gut bacteria[72], was upregulated in both the single *luxS* biofilms (Table 1) and *luxS* co-cultured with *B. fragilis* (Table 3). The upregulation of a phosphotransferase system component and *treA* (both in the same operon), likely enables increased utilisation of trehalose, providing an additional carbon source. Like glucose, trehalose acts as an osmoprotectant[73] and its presence within the cell may help maintain protein conformation during cellular dehydration. It is possible that trehalose plays a role in building *C. difficile* biofilms, as reported for *Candida* biofilms[74]. Our preliminary studies with exogenous trehalose levels similar

to those used by Collins *et al*. (2018) showed an inhibitory effect on biofilm formation by both WT *C. difficile* and *luxS*, although no differential effects were observed between *luxS* and WT (Fig. S9). However, further investigations into accumulation of trehalose within biofilms are required to clarify the role of trehalose in *luxS* mediated biofilm formation.

In conclusion, we report that *C. difficile* LuxS/AI-2 may play a key role in building *C. difficile* communities through mediating prophage induction, and subsequent accumulation of eDNA. In mixed communities, *C. difficile* AI-2 likely signals to *B. fragilis* to induce an altered metabolic response, enabling it to outgrow *C. difficile*. Further studies are required to understand the precise AI-2 sensing pathways involved.

Materials and Methods

Bacterial strains and media. Two bacterial species were used in this study – *C. difficile* strain: B1/NAP1/027 R20291 (isolated from the Stoke Mandeville outbreak in 2004 and 2005), and *Bacteroides fragilis* (a clinical isolate from a biliary stent kindly provided by Dr Claudia Vuotto and Dr Gianfranco Donelli, Rome). A *luxS* Clostron R20291 mutant described previously in Dapa *et al*.[27] was used in this study. Both species were cultured under anaerobic conditions (80% N_2, 10% CO_2, 10% H_2) at 37 °C in an anaerobic workstation (Don Whitley, United Kingdom) in BHIS, supplemented with L-Cysteine (0.1% w/v; Sigma, United Kingdom), yeast extract (5 g/l; Oxoid) and glucose (0.1 M).

Vibrio harveyi strain: BB170 was used to measure AI-2. *V. harveyi* strains were cultured in aerobic conditions at 30 °C in Lysogeny broth (LB) supplemented with kanamycin (50 µg/ml).

Biofilm formation assay. Biofilms were grown as per the previously published protocol[27]. Overnight cultures of *C. difficile* were diluted 1:100 in fresh BHIS with 0.1 M glucose. 1 ml aliquots were pipetted into 24-well tissue culture treated polystyrene plates (Costar), and incubated under anaerobic condition at 37 °C, for 6–120 h. Tissue culture plates were pre-incubated for 48 h prior to use. The plates were wrapped with parafilm to prevent liquid evaporation.

Measurement of biofilm biomass. Biofilm biomass was measured using crystal violet (CV)[27]. After the required incubation, each well of the 24-well plate was washed with sterile phosphate buffer saline (PBS) and allowed to dry for a minimum of 10 mins. The biofilm was stained using 1 ml of filter-sterilised 0.2% CV and incubated for 30 mins at 37 °C, in anaerobic conditions. The CV was removed from each well, and wells were subsequently washed twice with sterile PBS. The dye was extracted by incubated with 1 ml methanol for 30 mins at room temperature in aerobic conditions. The methanol-extracted dye was diluted 1:1, 1:10 or 1:100 and OD_{570} was measured with a spectrophotometer (BMG Labtech, UK).

For bacterial cell counts from the biofilm, the planktonic phase was removed and wells were washed once using sterile PBS. The adherent biofilms were then detached by scrapping with a sterile pipette tip and re-suspended into 1 ml PBS. Serial dilutions were made and plated onto BHIS plates to determine the CFU present in the biofilm.

Co-culture biofilm assay. For generation of co-culture biofilms, both *C. difficile* and *B. fragilis* were diluted to an OD_{600} of 1. Both species were diluted 1:100 into fresh BHIS with 0.1 M glucose. Biofilms assays were performed as described above and measured by a combination of CV staining and CFU. To distinguish between *C. difficile* and *B. fragilis*, serial dilutions used for determining CFU were plated on BHIS plates additionally supplemented with *C. difficile* selective supplement (Oxoid, UK). Colonies can be differentiated by size and colony morphology as *B. fragilis* form very small colonies.

Exogenous addition of DPD. To analyse the potential signalling role of AI-2, biofilm assays were performed as described above in BHIS with 0.1 M glucose containing 1 nM, 10 nM, 100 nM, or 1 µM of chemically synthesised, exogenous 4,5-Dihydroxy-2,3-pentanedione (Omm Scientific, Texas USA) for both *C. difficile* WT and LuxS. BHIS with 0.1 M glucose was used as a control. Samples were washed and stained with 0.2% CV at either 24 h or 72 h.

AI-2 Assay. The AI-2 bioluminescence assay was carried out essentially as described by Bassler *et al*. 1993[75]. The *V. harveyi* reporter strain BB170 was grown overnight in LB medium before being diluted 1: 5000 in Autoinducer Bioassay (AB) medium containing 10% (v/v) cell-free conditioned medium collected from either planktonic or biofilm *C. difficile* cultures (in BHI) and allowed to grow at 30 °C with shaking. AB medium containing 10% (v/v) from *V. harveyi* BB120 was used as a positive control, and 10% (v/v) sterile BHI medium as a blank. Luminescence was measured every hour using a SPECTROstar Omega plate reader. Induction of luminescence was taken at the time when there was maximal difference between the positive and negative controls (usually 2–5 h) and is expressed as a percentage of the induction observed in the positive control.

RNA-seq. Biofilms were grown for 18 h in BHIS + glucose, supernatants were removed and attached biofilms were washed with 1 ml PBS. Biofilms were disrupted and RNA was extracted using Trizol (Invitrogen, UK). 5 µg of extracted RNA was treated with RiboZERO™ (Illumina, UK) according to the manufacturer's protocol to deplete rRNA. cDNA libraries were prepared using TruSEQ LT (Illumina, UK) according to the manufacturer's instructions. Briefly, samples were end-repaired, mono-adenylated, ligated to index/adaptors. Libraries were quantified by bioanalyzer and fluorometer assay. The final cDNA library was prepared to a concentration of 10–12 pM and sequenced using paired end technology using a version-3 150-cycle kit on an Illumina MiSeq™ (Illumina, UK).

RNA-seq analysis. The paired-end sequencing reads from RNA-seq experiments were mapped against the appropriate reference genome (NC_013316 for *C. difficile* and a de novo assembly using RNA SPAdes v3.9 with default settings[76] from the RNA-sequence reads for *B. fragilis* [Accession number PRJEB29695). The first read was flipped into the correct orientation using seqtk v1.3 (https://github.com/lh3/seqtk) and the reads were mapped against the reference genome using BWA v0.7.5 with the 'mem' alignment algorithm[77]. BAM files were manipulated with Samtools v0.1.18 using the 'view' and 'sort' settings[77]. Sorted BAM and GFF (general feature format) files were inputted into the coverageBed tool v2.27.0 with default settings[78] to gain abundance of each genomic feature. The R package DESeq2 was used with default settings to calculate differential gene expression using a negative binomial distribution model[42]. The data was filtered by applying a cut-off of 1.6 for the fold change and 0.05 for the adjusted *p*-value. All sequencing reads were submitted to the European Bioinformatics Institute (Accession numbers E-MTAB-7486, E-MTAB-7523 and PRJEB29695).

As analysis by BLAST (NCBI) demonstrated species specificity for mapping, co-culture samples were mapped to each species reference separately. Initial mapping of the *B. fragilis* strain to a published reference proved unsuccessful, offering a poor rate of alignment of 60%. As the *B. fragilis* strain has not been previously sequenced, and because we were not successful in generating high quality genome sequence, a reference was generated from RNA library of *B. fragilis* using the software rnaSPAdes v3.9[79] and annotated using Prokka v1.11 (default settings)[80]. The reads from each condition were mapped to their respective reference sequence using BWA v0.7.5 ('mem' algorithm)[77,81] and counted using coverageBed v2.27.0[78]. Metabolic pathways in *C. difficile* were identified using the KEGG mapper[82], a tool that identifies the function of genes in a published genome. As the *B. fragilis* strain used in this study does not have a published reference genome, blastKOALA[83] was used to search for gene homology within metabolic pathways. Heatmaps were generated from normalised gene expression data outputted from DESeq2, using the online tool Heatmapper[84] using the default settings.

PCR analysis. 16S PCRs were performed using the universal 16S rRNA bacterial primers 27F and 1392R (Table S2). Primers were constructed for prophage genes CDR20219_1208 and CDR20291_1436 (Table S2) to confirm the presence of prophage within *C. difficile* biofilms. PCR was carried out using Fusion High-Fidelity DNA polymerase (NEB, USA) following the manufacturer's protocol. Samples were heated to 95 °C for 5 mins followed by 35 cycles of: 95 °C for 30 seconds, 51 °C for 30 seconds and 72 °C for 30 seconds, after which samples were heated to 72 °C for 10 mins.

eDNA quantification. eDNA was extracted from *C. difficile* biofilms grown in a 24-well plate as described above, using a protocol described in Rice *et al.*[53]. Briefly, the plate was sealed with parafilm and chilled at 4 °C for 1 hour. 1 µl 0.5 M EDTA was added to each well and incubated at 4 °C for 5 mins. The medium was removed and biofilms were resuspended in 300 µl 50 mM TES buffer (50 mM Tris HCl/10 mM EDTA/500 mM NaCl). The OD_{600} was measured to determine biofilm biomass and the tubes were centrifuged at 4 °C at 18,000 g for 5 mins, and was used to normalise the eDNA values. 100 µl of supernatant was transferred to a tube of chilled TE buffer (10 mM Tris HCl/ 1 mM EDTA) on ice. DNA was extracted using an equal volume of phenol/chloroform/isoamyl alcohol three times. 3 volumes of ice-cold 100% ethanol and 1/10 volumes 3 M sodium acetate were added to the aqueous phase to precipitate the DNA. The DNA pellet was washed with 1 ml ice-cold 70% ethanol, dissolved in 20 µl TE buffer, quantified by Qubit fluorometer (Thermo Fisher).

Spore counts. To determine the number of spores, adherent biofilms were resuspended in PBS and treated at 65 °C for 25 mins as previously described[85]. Untreated and heat-treated samples were serial diluted and plated on BHIS and BHIS-TC agar (supplemented with 0.1% sodium taurocholate, Sigma-Aldrich, UK). No bacteria were obtained from the heat-treated samples plated on BHI (without sodium taurocholate). The CFU/ml obtained from heat-treated samples plated on BHIS-TC plates represent heat-resistant spores, and the CFU/ml obtained from untreated samples plated on BHIS plates represent the total cell counts.

Statistical analysis. All experiments were performed in triplicate, with at least three independent experiments performed. Paired or unpaired student's t-test was used to determine if differences between two groups were significant, and one way-ANOVA was used to compare multiple groups. Mann-Whitney U tests were used to compare non-parametric data. Fisher's exact t-test was used to confirm the enrichment of differently regulated genes in prophage regions.

References

1. Lessa, F. C. *et al.* Burden of *Clostridium difficile* infection in the United States. *N Engl J Med* **372**, 825–834, https://doi.org/10.1056/NEJMoa1408913 (2015).
2. Davies, K. A. *et al.* Underdiagnosis of *Clostridium difficile* across Europe: the *European*, multicentre, prospective, biannual, point-prevalence study of *Clostridium difficile* infection in hospitalised patients with diarrhoea (EUCLID). *Lancet Infect Dis* **14**, 1208–1219, https://doi.org/10.1016/S1473-3099(14)70991-0 (2014).
3. Gravel, D. *et al.* Health care-associated *Clostridium difficile* infection in adults admitted to acute care hospitals in Canada: a Canadian Nosocomial Infection Surveillance Program Study. *Clin Infect Dis* **48**, 568–576, https://doi.org/10.1086/596703 (2009).
4. Collins, D. A., Selvey, L. A., Celenza, A. & Riley, T. V. Community-associated *Clostridium difficile* infection in emergency department patients in Western Australia. *Anaerobe* **48**, 121–125, https://doi.org/10.1016/j.anaerobe.2017.08.008 (2017).
5. Barbut, F. *et al.* Epidemiology of recurrences or reinfections of *Clostridium difficile*-associated diarrhea. *J Clin Microbiol* **38**, 2386–2388 (2000).
6. Rupnik, M., Wilcox, M. H. & Gerding, D. N. *Clostridium difficile* infection: new developments in epidemiology and pathogenesis. *Nat Rev Microbiol* **7**, 526–536, https://doi.org/10.1038/nrmicro2164 (2009).
7. Smits, W. K., Lyras, D., Lacy, D. B., Wilcox, M. H. & Kuijper, E. J. *Clostridium difficile* infection. *Nat Rev Dis Primers* **2**, 16020, https://doi.org/10.1038/nrdp.2016.20 (2016).
8. Hopkins, M. J. & Macfarlane, G. T. Changes in predominant bacterial populations in human faeces with age and with *Clostridium difficile* infection. *J Med Microbiol* **51**, 448–454, https://doi.org/10.1099/0022-1317-51-5-448 (2002).

9. Manges, A. R. *et al*. Comparative metagenomic study of alterations to the intestinal microbiota and risk of nosocomial *Clostridium difficile*-associated disease. *J Infect Dis* **202**, 1877–1884, https://doi.org/10.1086/657319 (2010).
10. Seekatz, A. M. *et al*. Recovery of the gut microbiome following fecal microbiota transplantation. *mBio* **5**, e00893–00814, https://doi.org/10.1128/mBio.00893-14 (2014).
11. Schubert, A. M. *et al*. Microbiome data distinguish patients with *Clostridium difficile* infection and non-C. difficile-associated diarrhea from healthy controls. *mBio* **5**, e01021–01014, https://doi.org/10.1128/mBio.01021-14 (2014).
12. Khoruts, A., Dicksved, J., Jansson, J. K. & Sadowsky, M. J. Changes in the composition of the human fecal microbiome after bacteriotherapy for recurrent *Clostridium difficile*-associated diarrhea. *J Clin Gastroenterol* **44**, 354–360, https://doi.org/10.1097/MCG.0b013e3181c87e02 (2010).
13. Hamilton, M. J., Weingarden, A. R., Unno, T., Khoruts, A. & Sadowsky, M. J. High-throughput DNA sequence analysis reveals stable engraftment of gut microbiota following transplantation of previously frozen fecal bacteria. *Gut Microbes* **4**, 125–135, https://doi.org/10.4161/gmic.23571 (2013).
14. Britton, R. A. & Young, V. B. Role of the intestinal microbiota in resistance to colonization by *Clostridium difficile*. *Gastroenterology* **146**, 1547–1553, https://doi.org/10.1053/j.gastro.2014.01.059 (2014).
15. Sorg, J. A. & Sonenshein, A. L. Bile salts and glycine as cogerminants for *Clostridium difficile* spores. *J Bacteriol* **190**, 2505–2512, https://doi.org/10.1128/JB.01765-07 (2008).
16. Buffie, C. G. *et al*. Precision microbiome reconstitution restores bile acid mediated resistance to *Clostridium difficile*. *Nature* **517**, 205–208, https://doi.org/10.1038/nature13828 (2015).
17. Ferreyra, J. A. *et al*. Gut microbiota-produced succinate promotes *C. difficile* infection after antibiotic treatment or motility disturbance. *Cell Host Microbe* **16**, 770–777, https://doi.org/10.1016/j.chom.2014.11.003 (2014).
18. Ng, K. M. *et al*. Microbiota-liberated host sugars facilitate post-antibiotic expansion of enteric pathogens. *Nature* **502**, 96–99, https://doi.org/10.1038/nature12503 (2013).
19. Kuehne, S. A. *et al*. The role of toxin A and toxin B in *Clostridium difficile* infection. *Nature* **467**, 711–713, https://doi.org/10.1038/nature09397 (2010).
20. Lyras, D. *et al*. Toxin B is essential for virulence of *Clostridium difficile*. *Nature* **458**, 1176–1179, https://doi.org/10.1038/nature07822 (2009).
21. Voth, D. E. & Ballard, J. D. *Clostridium difficile* toxins: mechanism of action and role in disease. *Clin Microbiol Rev* **18**, 247–263, https://doi.org/10.1128/CMR.18.2.247-263.2005 (2005).
22. Merrigan, M. M. *et al*. Surface-layer protein A (SlpA) is a major contributor to host-cell adherence of *Clostridium difficile*. *PloS one* **8**, e78404, https://doi.org/10.1371/journal.pone.0078404 (2013).
23. Waligora, A. J. *et al*. Characterization of a cell surface protein of *Clostridium difficile* with adhesive properties. *Infect Immun* **69**, 2144–2153, https://doi.org/10.1128/IAI.69.4.2144-2153.2001 (2001).
24. Kovacs-Simon, A. *et al*. Lipoprotein CD0873 is a novel adhesin of *Clostridium difficile*. *J Infect Dis* **210**, 274–284, https://doi.org/10.1093/infdis/jiu070 (2014).
25. Barketi-Klai, A., Hoys, S., Lambert-Bordes, S., Collignon, A. & Kansau, I. Role of fibronectin-binding protein A in *Clostridium difficile* intestinal colonization. *J Med Microbiol* **60**, 1155–1161, https://doi.org/10.1099/jmm.0.029553-0 (2011).
26. Tasteyre, A., Barc, M.-C., Collignon, A., Boureau, H. & Karjalainen, T. Role of FliC and FliD Flagellar Proteins of *Clostridium difficile* in Adherence and Gut Colonization. *Infection and Immunity* **69**, 7937–7940, https://doi.org/10.1128/iai.69.12.7937-7940.2001 (2001).
27. Dapa, T. *et al*. Multiple factors modulate biofilm formation by the anaerobic pathogen *Clostridium difficile*. *J Bacteriol* **195**, 545–555, https://doi.org/10.1128/JB.01980-12 (2013).
28. Dawson, L. F., Valiente, E., Faulds-Pain, A., Donahue, E. H. & Wren, B. W. Characterisation of *Clostridium difficile* biofilm formation, a role for Spo0A. *PloS one* **7**, e50527, https://doi.org/10.1371/journal.pone.0050527 (2012).
29. Mathur, H., Rea, M. C., Cotter, P. D., Hill, C. & Ross, R. P. The efficacy of thuricin CD, tigecycline, vancomycin, teicoplanin, rifampicin and nitazoxanide, independently and in paired combinations against *Clostridium difficile* biofilms and planktonic cells. *Gut Pathog* **8**, 20, https://doi.org/10.1186/s13099-016-0102-8 (2016).
30. Semenyuk, E. G. *et al*. Spore formation and toxin production in *Clostridium difficile* biofilms. *PloS one* **9**, e87757, https://doi.org/10.1371/journal.pone.0087757 (2014).
31. Li, Y. H. & Tian, X. Quorum sensing and bacterial social interactions in biofilms. *Sensors (Basel)* **12**, 2519–2538, https://doi.org/10.3390/s120302519 (2012).
32. Antunes, L. C., Ferreira, R. B., Buckner, M. M. & Finlay, B. B. Quorum sensing in bacterial virulence. *Microbiology* **156**, 2271–2282, https://doi.org/10.1099/mic.0.038794-0 (2010).
33. Vendeville, A., Winzer, K., Heurlier, K., Tang, C. M. & Hardie, K. R. Making 'sense' of metabolism: autoinducer-2, LuxS and pathogenic bacteria. *Nat Rev Microbiol* **3**, 383–396, https://doi.org/10.1038/nrmicro1146 (2005).
34. Rezzonico, F. & Duffy, B. Lack of genomic evidence of AI-2 receptors suggests a non-quorum sensing role for luxS in most bacteria. *BMC Microbiol* **8**, 154, https://doi.org/10.1186/1471-2180-8-154 (2008).
35. Auger, S., Krin, E., Aymerich, S. & Gohar, M. Autoinducer 2 affects biofilm formation by *Bacillus cereus*. *Appl Environ Microbiol* **72**, 937–941, https://doi.org/10.1128/AEM.72.1.937-941.2006 (2006).
36. De Araujo, C., Balestrino, D., Roth, L., Charbonnel, N. & Forestier, C. Quorum sensing affects biofilm formation through lipopolysaccharide synthesis in *Klebsiella pneumoniae*. *Res Microbiol* **161**, 595–603, https://doi.org/10.1016/j.resmic.2010.05.014 (2010).
37. Hardie, K. R. & Heurlier, K. Establishing bacterial communities by 'word of mouth': LuxS and autoinducer 2 in biofilm development. *Nat Rev Microbiol* **6**, 635–643, https://doi.org/10.1038/nrmicro1916 (2008).
38. Huang, Z. *et al*. luxS-based quorum-sensing signaling affects Biofilm formation in *Streptococcus mutans*. *J Mol Microbiol Biotechnol* **17**, 12–19, https://doi.org/10.1159/000159193 (2009).
39. Karim, M. M. *et al*. LuxS affects biofilm maturation and detachment of the periodontopathogenic bacterium *Eikenella corrodens*. *J Biosci Bioeng* **116**, 313–318, https://doi.org/10.1016/j.jbiosc.2013.03.013 (2013).
40. Carter, G. P., Purdy, D., Williams, P. & Minton, N. P. Quorum sensing in *Clostridium difficile*: analysis of a luxS-type signalling system. *J Med Microbiol* **54**, 119–127 (2005).
41. Lee, A. S. & Song, K. P. LuxS/autoinducer-2 quorum sensing molecule regulates transcriptional virulence gene expression in *Clostridium difficile*. *Biochem Biophys Res Commun* **335**, 659–666, https://doi.org/10.1016/j.bbrc.2005.07.131 (2005).
42. Love, M. I., Huber, W. & Anders, S. Moderated estimation of fold change and dispersion for RNA-seq data with DESeq2. *Genome Biol* **15**, 550, https://doi.org/10.1186/s13059-014-0550-8 (2014).
43. Arndt, D. *et al*. PHASTER: a better, faster version of the PHAST phage search tool. *Nucleic Acids Res* **44**, W16–21, https://doi.org/10.1093/nar/gkw387 (2016).
44. Zhou, Y., Liang, Y., Lynch, K. H., Dennis, J. J. & Wishart, D. S. PHAST: a fast phage search tool. *Nucleic Acids Res* **39**, W347–352, https://doi.org/10.1093/nar/gkr485 (2011).
45. Bassler, B. L., Greenberg, E. P. & Stevens, A. M. Cross-species induction of luminescence in the quorum-sensing bacterium *Vibrio harveyi*. *J Bacteriol* **179**, 4043–4045 (1997).
46. Goldberg, E. *et al*. The correlation between *Clostridium-difficile* infection and human gut concentrations of Bacteroidetes phylum and clostridial species. *Eur J Clin Microbiol Infect Dis* **33**, 377–383, https://doi.org/10.1007/s10096-013-1966-x (2014).

47. Andrews, S. C., Robinson, A. K. & Rodriguez-Quinones, F. Bacterial iron homeostasis. *FEMS Microbiol Rev* **27**, 215–237, https://doi.org/10.1016/S0168-6445(03)00055-X (2003).
48. Zhu, J. & Mekalanos, J. J. Quorum sensing-dependent biofilms enhance colonization in *Vibrio cholerae*. *Dev Cell* **5**, 647–656 (2003).
49. Sakuragi, Y. & Kolter, R. Quorum-sensing regulation of the biofilm matrix genes (pel) of *Pseudomonas aeruginosa*. *J Bacteriol* **189**, 5383–5386, https://doi.org/10.1128/JB.00137-07 (2007).
50. Solano, C., Echeverz, M. & Lasa, I. Biofilm dispersion and quorum sensing. *Curr Opin Microbiol* **18**, 96–104, https://doi.org/10.1016/j.mib.2014.02.008 (2014).
51. Wolf, T., Kammer, P., Brunke, S. & Linde, J. Two's company: studying interspecies relationships with dual RNA-seq. *Curr Opin Microbiol* **42**, 7–12, https://doi.org/10.1016/j.mib.2017.09.001 (2018).
52. Ibanez de Aldecoa, A. L., Zafra, O. & Gonzalez-Pastor, J. E. Mechanisms and Regulation of Extracellular DNA Release and Its Biological Roles in Microbial Communities. *Front Microbiol* **8**, 1390, https://doi.org/10.3389/fmicb.2017.01390 (2017).
53. Rice, K. C. *et al*. The cidA murein hydrolase regulator contributes to DNA release and biofilm development in *Staphylococcus aureus*. *Proc Natl Acad Sci USA* **104**, 8113–8118, https://doi.org/10.1073/pnas.0610226104 (2007).
54. Brackman, G. *et al*. The Quorum Sensing Inhibitor Hamamelitannin Increases Antibiotic Susceptibility of *Staphylococcus aureus* Biofilms by Affecting Peptidoglycan Biosynthesis and eDNA Release. *Sci Rep* **6**, 20321, https://doi.org/10.1038/srep20321 (2016).
55. Svensson, S. L., Pryjma, M. & Gaynor, E. C. Flagella-mediated adhesion and extracellular DNA release contribute to biofilm formation and stress tolerance of *Campylobacter jejuni*. *PloS one* **9**, e106063, https://doi.org/10.1371/journal.pone.0106063 (2014).
56. Nale, J. Y. *et al*. Diverse temperate bacteriophage carriage in *Clostridium difficile* 027 strains. *PloS one* **7**, e37263, https://doi.org/10.1371/journal.pone.0037263 (2012).
57. Stabler, R. A. *et al*. Comparative genome and phenotypic analysis of *Clostridium difficile* 027 strains provides insight into the evolution of a hypervirulent bacterium. *Genome Biol* **10**, R102, https://doi.org/10.1186/gb-2009-10-9-r102 (2009).
58. Sekulovic, O. & Fortier, L. C. Global transcriptional response of *Clostridium difficile* carrying the CD38 prophage. *Appl Environ Microbiol* **81**, 1364–1374, https://doi.org/10.1128/AEM.03656-14 (2015).
59. Secor, P. R. *et al*. Biofilm assembly becomes crystal clear - filamentous bacteriophage organize the *Pseudomonas aeruginosa* biofilm matrix into a liquid crystal. *Microb Cell* **3**, 49–52, https://doi.org/10.15698/mic2016.01.475 (2015).
60. Rossmann, F. S. *et al*. Phage-mediated dispersal of biofilm and distribution of bacterial virulence genes is induced by quorum sensing. *PLoS Pathog* **11**, e1004653, https://doi.org/10.1371/journal.ppat.1004653 (2015).
61. Pantaleon, V. *et al*. *Clostridium difficile* forms variable biofilms on abiotic surface. *Anaerobe*, https://doi.org/10.1016/j.anaerobe.2018.05.006 (2018).
62. Yoon, S. *et al*. Bile salt hydrolase-mediated inhibitory effect of Bacteroides ovatus on growth of *Clostridium difficile*. *J Microbiol* **55**, 892–899, https://doi.org/10.1007/s12275-017-7340-4 (2017).
63. Poquet, I. *et al*. *Clostridium difficile* Biofilm: Remodeling Metabolism and Cell Surface to Build a Sparse and Heterogeneously Aggregated Architecture. *Front Microbiol* **9**, 2084, https://doi.org/10.3389/fmicb.2018.02084 (2018).
64. Macy, J. M., Ljungdahl, L. G. & Gottschalk, G. Pathway of succinate and propionate formation in *Bacteroides fragilis*. *J Bacteriol* **134**, 84–91 (1978).
65. Bruckner, R. & Titgemeyer, F. Carbon catabolite repression in bacteria: choice of the carbon source and autoregulatory limitation of sugar utilization. *FEMS Microbiol Lett* **209**, 141–148, https://doi.org/10.1111/j.1574-6968.2002.tb11123.x (2002).
66. Wagegg, W. & Braun, V. Ferric citrate transport in *Escherichia coli* requires outer membrane receptor protein fecA. *J Bacteriol* **145**, 156–163 (1981).
67. Kortman, G. A., Raffatellu, M., Swinkels, D. W. & Tjalsma, H. Nutritional iron turned inside out: intestinal stress from a gut microbial perspective. *FEMS Microbiol Rev* **38**, 1202–1234, https://doi.org/10.1111/1574-6976.12086 (2014).
68. Federle, M. J. & Bassler, B. L. Interspecies communication in bacteria. *J Clin Invest* **112**, 1291–1299, https://doi.org/10.1172/JCI20195 (2003).
69. Antunes, L. C. *et al*. Bacteroides species produce *Vibrio harveyi* autoinducer 2-related molecules. *Anaerobe* **11**, 295–301, https://doi.org/10.1016/j.anaerobe.2005.03.003 (2005).
70. Hsiao, A. *et al*. Members of the human gut microbiota involved in recovery from *Vibrio cholerae* infection. *Nature* **515**, 423–426, https://doi.org/10.1038/nature13738 (2014).
71. Thompson, J. A., Oliveira, R. A., Djukovic, A., Ubeda, C. & Xavier, K. B. Manipulation of the quorum sensing signal AI-2 affects the antibiotic-treated gut microbiota. *Cell Rep* **10**, 1861–1871, https://doi.org/10.1016/j.celrep.2015.02.049 (2015).
72. Collins, J. *et al*. Dietary trehalose enhances virulence of epidemic *Clostridium difficile*. *Nature* **553**, 291–294, https://doi.org/10.1038/nature25178 (2018).
73. Tanghe, A., Van Dijck, P. & Thevelein, J. M. Determinants of freeze tolerance in microorganisms, physiological importance, and biotechnological applications. *Adv Appl Microbiol* **53**, 129–176 (2003).
74. Zhu, Z. *et al*. Time course analysis of *Candida albicans* metabolites during biofilm development. *J Proteome Res* **12**, 2375–2385, https://doi.org/10.1021/pr300447k (2013).
75. Bassler, B. L., Wright, M., Showalter, R. E. & Silverman, M. R. Intercellular signalling in *Vibrio harveyi*: sequence and function of genes regulating expression of luminescence. *Mol Microbiol* **9**, 773–786 (1993).
76. Bushmanova E. A. D., Lapidus, A. & Przhibelskiy, A. D. rnaSPAdes: a de novo transcriptome assembler and its application to RNA-Seq data. *BioRxiv*, https://doi.org/10.1101/420208 (2018).
77. Li, H. & Durbin, R. Fast and accurate short read alignment with Burrows-Wheeler transform. *Bioinformatics* **25**, 1754–1760, https://doi.org/10.1093/bioinformatics/btp324 (2009).
78. Quinlan, A. R. BEDTools: The Swiss-Army Tool for Genome Feature Analysis. *Curr Protoc Bioinformatics* **47**, 11 12 11–34, https://doi.org/10.1002/0471250953.bi1112s47 (2014).
79. Bankevich, A. *et al*. SPAdes: a new genome assembly algorithm and its applications to single-cell sequencing. *J Comput Biol* **19**, 455–477, https://doi.org/10.1089/cmb.2012.0021 (2012).
80. Seemann, T. Prokka: rapid prokaryotic genome annotation. *Bioinformatics* **30**, 2068–2069, https://doi.org/10.1093/bioinformatics/btu153 (2014).
81. Li, H. & Durbin, R. Fast and accurate long-read alignment with Burrows-Wheeler transform. *Bioinformatics* **26**, 589–595, https://doi.org/10.1093/bioinformatics/btp698 (2010).
82. Kanehisa, M. & Goto, S. KEGG: kyoto encyclopedia of genes and genomes. *Nucleic Acids Res* **28**, 27–30 (2000).
83. Kanehisa, M., Sato, Y. & Morishima, K. BlastKOALA and GhostKOALA: KEGG Tools for Functional Characterization of Genome and Metagenome Sequences. *J Mol Biol* **428**, 726–731, https://doi.org/10.1016/j.jmb.2015.11.006 (2016).
84. Babicki, S. *et al*. Heatmapper: web-enabled heat mapping for all. *Nucleic Acids Res* **44**, W147–153, https://doi.org/10.1093/nar/gkw419 (2016).
85. Fimlaid, K. A., Jensen, O., Donnelly, M. L., Siegrist, M. S. & Shen, A. Regulation of *Clostridium difficile* Spore Formation by the SpoIIQ and SpoIIIA Proteins. *PLoS Genet* **11**, e1005562, https://doi.org/10.1371/journal.pgen.1005562 (2015).

Acknowledgements

We thank Gianfranco Donelli, and Claudia Vuotto, Microbial Biofilm Laboratory, IRCCS Fondazione Santa Lucia, Italy for providing the *Bacteroides fragilis* isolate and Prof Paul Williams, University of Nottingham for providing the *Vibrio harveyi* strain BB170. This was in part supported by a Seed grant from the Wellcome Warwick Quantitative Biomedicine Programme (Institutional Strategic Support Fund: 105627/Z/14/Z). We thank the Biotechnology and Biological Sciences Research Council (BBSRC) funded Midland Integrative Biosciences Training Partnership (MIBTP) studentships to LF and SR.

Author Contributions

R.S., L.F., S.J. designed and performed experiments for this study. A.M. and R.S. performed sequencing data analysis. R.S. and M.U. wrote the main manuscript and all authors reviewed the manuscript.

Additional Information

Supplementary information accompanies this paper at https://doi.org/10.1038/s41598-019-46143-6.

Competing Interests: The authors declare no competing interests.

Publisher's note: Springer Nature remains neutral with regard to jurisdictional claims in published maps and institutional affiliations.